Kinetic and chemorheological modeling of thermosetting polyurethanes obtained from an epoxidized soybean oil polyol crosslinked with glycerin

Franco Armanasco[1] | **Sebastián D'hers**[2] | **Leonel Matías Chiacchiarelli**[1]

[1]Instituto de Tecnología de Polímeros y Nanotecnología (ITPN), CONICET-UBA, CABA, Argentina

[2]Instituto Tecnológico de Buenos Aires, Departamento de Ingeniería Mecánica, CABA, Argentina

Correspondence
Leonel Matías Chiacchiarelli, Instituto de Tecnología de Polímeros y Nanotecnología (ITPN), CONICET-UBA, Av. Gral. Las Heras 2214, C1126 CABA, Argentina.
Email: lchiacchiarelli@itba.edu.ar

Funding information
Agencia Nacional de Promoción Científica y Tecnológica, Grant/Award Numbers: PICT2015 N0475, PIP 2015 N0425; CONICET

Abstract

Thermosetting polyurethanes were obtained using an aromatic isocyanate and a hydrophobic polyol formulation obtained from epoxidized soybean oil (ESO) crosslinked with glycerin. A systematic DSC analysis of the effect of catalyst type, crosslinker concentration, isocyanate index and ESO crystallization on cure kinetics was conducted. The combination of a stannic catalyst at 0.2 wt% and glycerin at 20 wt% produced a cure kinetics governed by an autocatalytic heat flow where vitrification played a key role in the formation of chemical bonds. The evolution of T_g as a function of conversion, which followed Di-Benedetto's predictions, supported the hypothesis that vitrification was a preponderant phenomenon during cure. Dynamic Mechanical Analysis (DMA) of a post-cured sample revealed a Tg centered at 220°C, whereas quasi-static flexural mechanical tests shown a flexural modulus of 2.14 GPa and a flexural strength of 99.4 MPa. Rheological experiments at isothermal conditions supported the hypothesis that vitrification played a key role in the evolution of apparent viscosity. A master model using Kim-Macosko equations was obtained for the proposed formulation. The results presented in this work will serve to further extend the use of biobased polymers applied in the polymer composite industry.

KEYWORDS

chemorheology, cure kinetics, epoxidized soybean oil, epoxidized soybean oilglycerin, thermosetting polyurethane

1 | INTRODUCTION

The search for sustainable and environmental-friendly solutions within the polyurethane industry has fueled scientific and industrial activities, which emphasize the replacement of fossil-fuel precursors with renewable ones.[1] One of the most relevant initiatives in this regard is the development of polyols from vegetable oils.[2–7] Within the Americas region, soybean-oil based polyols are currently being developed both in industry and in scientific laboratories with the general objective to partially or fully replace petroleum-based polyols. Thermosetting polymers are ubiquitous for the development of polymer composites, however, a highly crosslinked network is a requirement to achieve that goal.[8] In polyurethanes, this means that highly functional polyols as well as isocyanates are mandatory. As we have already pointed out in the previous publication,[9] the synthesis of high hydroxide number (OH#) biobased polyols combined with a suitable functionality (>3.0) and low apparent viscosity (< 2000 cp) represents a challenge within this field. However, these polyols have a key property which renders it suitable for thermosetting

applications, that is, hydrophobicity. Epoxidation of soybean-oil is a frequent intermediate synthesis route to obtain polyols with low OH#.[10–12] A slight change of temperature[10–15] within the synthesis protocol can lead to reduced epoxidation efficiencies, giving rise to a polyol with a low OH#, good functionality and relatively low apparent viscosity.[9] In addition, the presence of oxirane moieties as well as low polar fatty ester chains renders the polyol a high hydrophobic character. It is known that polyurethane formulations are prone to the formation of gasses during cure.[16] Interestingly, a hydrophobic polyol can be extremely useful to circumvent this issue, allowing the development of a thermosetting which can potentially be applied to polymer composites. Introducing this requirement in the analysis and taking into account that these polyols have an OH# within the order of 150 mg KOH. mg^{-1} and functionalities of around 2.9, then, it is essential to have a crosslinker to develop a suitable formulation. We propose glycerin to achieve this goal. Being a byproduct of the biodiesel industry makes this biobased crosslinker a key component to improve the thermomechanical properties of the final polymer. Even though glycerin has been used previously as a crosslinker as well as a starter for polyol synthesis,[17–20] the authors have not found any study using the formulation proposed in this study.

The development of new applications based on innovative thermoset polymers is strongly correlated to the understanding of its chemorheological behavior.[21–23] Obtaining a chemorheological master model[24–27] is a key prerequisite for the successful application of polymers in advanced applications. For example, polymer composite prepregs[28] represent a material of choice for advanced applications in aeronautics as well as aerospace applications.[28,29] Taking into account that the control and evolution of chemical conversion is a key issue for the development of prepregs, it is crucial to use chemorheological master models for that purpose. This, in turn, helps to avoid costly experiments whose sole purpose is to obtain an empirical solution to the problem. Even though several studies have been conducted to understand the chemorheological behavior of polyurethane thermosets,[24,30–35] the authors have not found any focusing on thermosets synthesized from soybean oil.

A key issue for the development of a TsPU formulation is the proper selection of catalyst type and concentration. If the main objective is to develop a thermosetting polyurethane, then it is desirable that the catalyst should selectively promote the formation of urethane or other covalent bonds (gelling chemical reactions); while simultaneously avoiding the formation of CO_2(g), which is caused mainly by the reaction of isocyanate with water (blowing reaction). Organotin compounds, such as stannous octoate and dibutyltin dilaurate (DBTDL), are currently widely employed in industry to this effect.[36] However, the main drawback of such catalysts are associated with increasing the toxicity of the resultant polyurethane formulation, particularly for biomedical applications. Organocatalysts[37] have a great potential to replace organotin compounds, however, their availability in industry is still limited to niche applications. Tertiary amines, such as DMCHA, have also been widely employed to alleviate this effect, however, its selectivity toward blowing reactions is much higher than gelling reactions. This represents a serious drawback because TsPUs need to have very low porosity levels to achieve improved thermomechanical properties. When it comes to the concentration of the catalyst, the minimum value is usually associated with the minimum amount which is capable of bringing a change of the order of the chemical reaction taking place.[38] For the case of DBTDL, the early studies of Marciano et al.[38] have shown that a minimum concentration of 2.6 mol. m^{-3} was appropriate. On the other hand, the maximum value is usually defined as a function of the processing method. For example, for the case of spray polyurethane foams (SPF), moderate to high concentrations are necessary to achieve a fast surface adhesion of the foam. On the other hand, for the case of thermosets applied in the polymer composite industry, the processing window is usually deducted from chemoviscosity profiles.[39] For example, if infusion[40] is used as the manufacturing process, it might be argued that having an apparent viscosity below 1000 mPa.s is a key prerequisite for the successful application of a thermosetting polymer.[28] For this reason, we have reported the chemoviscosity profile of the proposed formulation (see Section 3.1.3).

In this work, a complete chemorheological analysis (master model) of a thermosetting polyurethane (TsPU) has been developed using differential scanning calorimetry (DSC) as well as rotational rheometry. The effect of catalyst type and concentration, crosslinker concentration, isocyanate index (NCO_{index}) as well as the polyol crystallization have been systematically incorporated in the model. Thermomechanical studies of uncured and post-cured samples using dynamical mechanical thermal analysis (DMA) and quasi-static flexural bending were performed.

2 | MATERIALS AND METHODS

2.1 | Materials and sample preparation procedures

The epoxidized soybean oil polyol (ESO) was obtained using an epoxidation protocol based on formic acid (Anedra, A.C.S. grade) as the carrier and hydrogen peroxide (Stanton, 30% vol.) as the oxidizer, following the procedure of the previous works.[10,13] The reactions were performed at isothermal conditions (50°C) using a RBD grade soybean oil provided by Molinos Rio de La Plata

TABLE 1 Polyurethane formulations used in this work

Formulation	Polyol (pbw)	Isocyanate (pbw)	Glycerin (pbw)	DMCHA (pbw)	DBTDL (pbw)	Isocyanate NCO_{index}
$TsPU_1$	100	36.6	–	–	–	1.11
$TsPU_2$	100	36.6	–	0.3	–	1.11
$TsPU_3$	100	36.6	–	0.6	–	1.11
$TsPU_4$	100	36.6	–	0.9	–	1.11
$TsPU_5$	100	36.6	–	–	0.2	1.11
$TsPU_6$	100	36.6	20	–	0.2	0.31
$TsPU_7$	100	126	20	–	0.2	1.05
$TsPU_8$	100	164	20	–	0.2	1.37

and by mixing initially the soybean oil with formic acid and subsequently adding the oxidizer at a rate of 2 ml. min^{-1}. The organic phase was extracted using ethyl acetate (Biopack, A.C.S. grade) and neutralization with a saturated solution of NaCl. Finally, the resultant polyol, from now on denominated SOYPOL, was degassed using a vacuum mixer for 2 h. The OH# of the resultant polyol (137 mg KOH mg^{-1}) was obtained using the guidelines of the test method A provided by the ASTM D4274. So as to avoid crystallization of the SOYPOL, the sample was heated in convection oven at 50°C for at least 1 h and slowly cooled after turning off the oven.

A polymeric methylene diphenyl diisocyanate (pMDI), denominated commercially as Suprasec 5005 (Huntsman), with an NCO number of 31.0 and a functionality of 2.7 was used to prepare all the thermosetting samples. Before use, the pMDI was degassed using a dispermat vacuum mixer at 30 mbar and stirring at 5300 rpm. Glycerin (Anedra, USP) with a functionality of 3.0 and OH# of 1800 mgKOH. mg^{-1} was used after degassing in a vacuum mixer. Dibutyltin dilaurate (95%, Sigma-Aldrich) and dimethylcyclohexylamine (99%, Huntsman) were used as catalysts.

The polyurethane formulations used in this work are reported in Table 1. A total of eight formulations were tested to analyze the effect of catalyst type, isocyanate index (NCO_{index}) and crosslinking. The general preparation procedure consisted first with the degassing of the components using the protocols described in the last paragraph. Then, samples of approximately 80 g were prepared by mixing all the components listed in Table 1 and by adding the pMDI as the final one. Finally, the sample was mixed at a speed of 7800 rpm at 30 mbar. It is important to highlight that, only for Section 3.1.3, the final addition of pMDI was performed using manual mixing. As already noticed in the previous studies,[41,42] the mixing intensity has a fundamental role in the reactivity of polyurethane formulations. DSC analysis performed with hand mixed samples of the $TSPU_7$ revealed the presence of both low- and high-temperature transitions, indicating that the mixing efficiency led to a probable reaction between the isocyanate radicals.

2.2 | Sample characterization techniques

Heat flow analysis was performed using a Shimadzu DSC-60 differential scanning calorimeter (DSC) equipped with Aluminum hermetic pans. The dynamic thermal cycles started at 25°C going up to 200°C at a scan rate of 2°C min^{-1}. Sample mass was typically within the order of 10 mg.

SOYPOL-induced crystallization experiments were conducted by introducing bulk samples (approximately 50 grams) in refrigerators at temperatures of 4°C and − 18°C. After a specific time (see Table 2), DSC analysis were performed following the thermal cycle described in the previous paragraph. The presence of melting endotherms was identified by measuring the temperature of the melting point (T_P) as well as analyzing the area under the curve of the endothermic event (endothermic enthalpy).

The kinetic experiments associated to the determination of the evolution of the Tg as a function of conversion were conducted using DSC analysis. Initially, the samples were subjected to an isothermal experiment at temperatures within the range of 30°C up to 70°C. Afterwards, the sample was subjected to a dynamic thermal cycle at conditions which were identical to the ones described in the first paragraph. This last thermal cycle was used to quantify the T_g associated with each isothermal experiment and, subsequently, to an specific conversion.

The chemorheological models developed in Section 3.1 were based on the heat flow evolved at what it is denominated as the cure region. To further understand this concept, the heat flow as a function of temperature for the $TsPU_7$ formulation is depicted in Figure 1. As it can be deduced from this graph, the initial steep heat flow rise is the region that we have used to develop

TABLE 2 Endothermic enthalpy as a function of exposure time/temperature for soy-based polyols.

Formulation	Storage time (days)	Temperature (°C)	Endothermic enthalpy (J/g)	T_p (°C)
SOYPOL	180	4	4.74	44
SOYPOL	90	−18	0.32	36

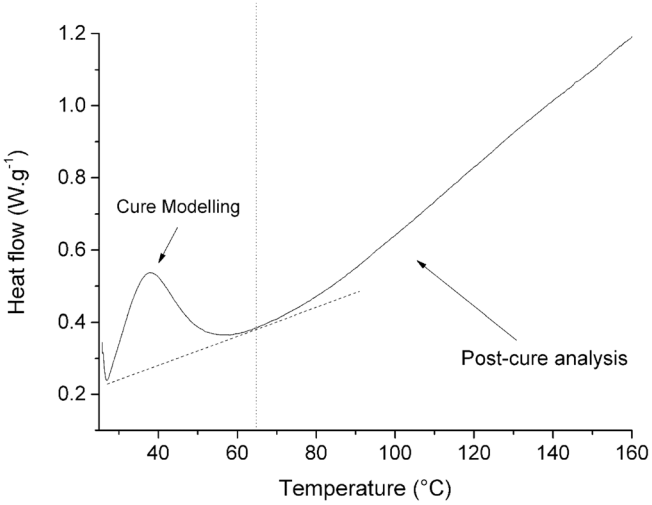

FIGURE 1 Heat flow as a function of temperature for the $TsPU_7$

the models. Hence, the conversion that we have used for the models developed in Equations (1)–(3) are strictly associated with this region. However, from Figure 1 it can also be deduced that, after the cure region, further exothermic heat flow was also measured. This heat flow is related to the post-cure analysis, where solid-state reactions are predominant. Due to the complex nature of polyurethane materials, it is logical to have further exothermic reactions which can encompass both the formation of additional chemical bonds as well as macromolecular rearrangements. This last characteristic is usually not a property of highly crosslinked thermosetting polymers (i.e. epoxy). In this regard, the concept of a single full cure cycle loses significance, because several molecular rearrangements are possible and each configuration produces a material with specific thermomechanical properties.

FTIR spectra were obtained using a Shimadzu IRAffinity-1 using attenuated total reflection (ATR) and absorption methods. The ATR method was used for liquid samples (uncured precursors). The ATR consisted of a Miracle single reflection device equipped with a ZnSe prism. Each spectrum was obtained by recording 50 scans in the range 4000–600 cm^{-1} with a resolution of 4 cm^{-1} at ambient temperature. The phenyl absorption band (centered at 1595 cm^{-1}) was used to normalize each spectra.

Dynamic Mechanical Thermal Analysis (DMA) was carried out using a Perkin & Elmer DMA 8000 equipment using the single cantilever bending fixture mode. The oscillation frequency was fixed at 1.0 Hz and the amplitude to 0.004 mm, previously selected from a strain scan at an ambient temperature. At least three samples were used to corroborate the reproducibility of the results. The sample dimensions were in the order of 10 mm in length, 8.8 mm in width and 1.8 mm in thickness. Each sample was subjected to two thermal cycles. The first one started at 25°C going up to 180°C at a scan rate of 3°C.min^{-1} and cooling again to ambient temperature. The second cycle was identical to the first one except that the final temperature was 240°C.

Rheological measurements were performed using a Brookfield Viscometer (Myr VR 3000) with a LV-3 stainless steel spindle. The measurements were performed at isothermal conditions with samples of approximately 150 grams using a stainless steel container submersed in an oil bath thermally controlled with a heating plate (Velp Scientific).

Quasi-static flexural mechanical tests were performed with an Instron 5985 following the guidelines of the standard ASTM D790. For each mechanical test, five samples were tested. The span to depth ratio was set to 16:1 and the speed of the flexural deformation was 0.1 mm.min^{-1}. These samples were post-cured in a horizontal forced air drying oven (Milab 101-2AB) using a thermal program which started at ambient temperature and went up to 70° C and 110°C at 10° C.min^{-1}. To allow for stabilization, heating stages which lasted 60′ were implemented at 20°C intervals.

3 | RESULTS AND DISCUSSION

3.1 | Chemorheological master model of the TsPU7 baseline formulation

3.1.1 | Cure kinetics of the TsPU7 formulation

The heat flow as a function of time for isothermal experiments during the cure of the $TsPU_7$ are depicted in Figure 2. The isothermal experiments were performed from 30°C all the way up to 70°C. First, it is important to emphasize that the time was synchronized with the start of the DSC isothermal experiment. The total time should also include the sampling preparation time, which is

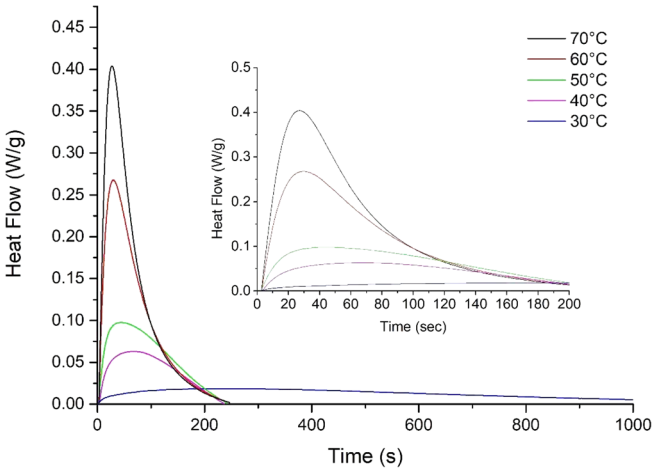

FIGURE 2 Heat flow as a function of time of the $TsPU_7$ formulation at isothermal conditions [Color figure can be viewed at wileyonlinelibrary.com]

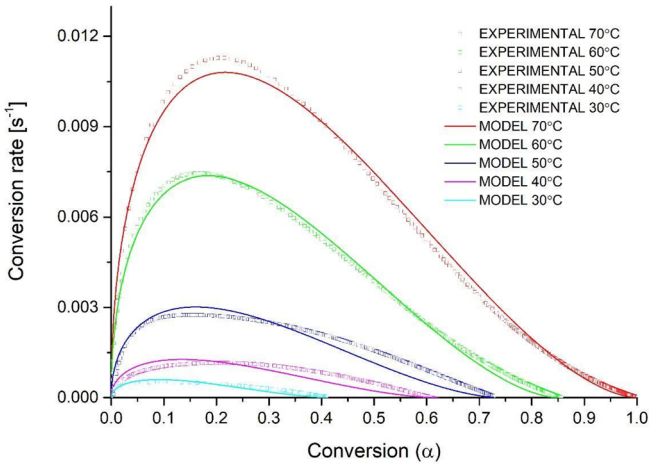

FIGURE 3 Conversion rate as a function of conversion comparing the experimental (dashed) and modeled (continuous) results of the $TsPU_7$-70°C formulation at isothermal conditions [Color figure can be viewed at wileyonlinelibrary.com]

TABLE 3 Cure enthalpy and maximum conversion at isothermal conditions for the $TSPU_7$.

Temperature (°C)	ΔH_{ISO} (J.g^{-1})	α_{max}
30	15 ± 0.6	0.42 ± 0.04
40	22.1 ± 1.93	0.62 ± 0.05
50	26.4 ± 2.7	0.74 ± 0.07
60	30.3 ± 2.15	0.85 ± 0.06
70	35.7 ± 3.31	1 ± 0.09

reported in the experimental section. This preparation time sets the limit of the maximum isothermal temperature, which was 70°C. For higher temperatures, the rise of the speed of the reaction would increase the exothermic heat flow to such an extent that its measurement would not be possible.

The total reaction enthalpy (ΔH_{ISO}) associated to each isothermal experiment is reported in Table 3. Taking into account the ΔH_T reported in Table 3, the maximum conversion (α_{max}) of each isothermal experiment was also calculated and reported in the same table. For example, at 30°C, a maximum conversion of 42% was achieved during cure. Clearly, this was an indication that vitrification took place and that a proper cure cycle should certainly include a post-cure cycle. On the other hand, the highest isothermal temperatures reached a full conversion, indicating that full cure was attained within this temperature range. It is important to emphasize what has already been explained in Section 2.2. When this thermosetting polymer is subjected to a post-cure cycle, further reactions will certainly take place. Hence, the concept of cure is highly associated to how the post-cure cycle was implemented.

The evolution of the maximum conversion as a function of cure temperature was found to follow a Boltzmann behavior according to the following equation:

$$\alpha_{max} = \frac{A}{1+\exp(\beta(T-T_{0.5}))} + B, \tag{1}$$

where A (−1.765), B (1.381), β (0.0349 °C^{-1}) were fitting parameters which affected the slope of the conversion curve and $T_{0.5}$ (33.99°C) was the absolute temperature (K) at which half conversion was achieved.

To better understand which phenomenological model was appropriate to predict the cure kinetics of the $TsPU_7$, the experimental data presented in Figure 2 was expressed as a function of conversion rate, where ΔH_{ISO} was the total enthalpic contribution associated to each isothermal experiment and ΔH_T represented the total enthalpy of the $TsPU_7$ formulation. The experiments expressed using conversion are reported in Figure 3. The shape of the curves presented in this figure were used to infer that an autocalytic phenomenological model should be implemented for the $TsPU_7$. In addition, taking into account that the maximum conversion increased as a function of temperature, it was also necessary to include vitrification in the model. Hence, the following equation was proposed,

$$\frac{d\alpha}{dt} = k\alpha^m(\alpha_{max}-\alpha)^n, \tag{2}$$

where n and m represented the reaction orders and $\underline{k}$ was the frequency factor that included an Arrhenius type temperature dependency and it was determined using the following equation,

Temperature (°C)	k (1/s)	*n*	*m*	*Ea*	Corr. coeff.
70	3.36×10^{-2}	1.70	0.47	2.71×10^{1}	0.9847
60	3.26×10^{-2}				
50	1.80×10^{-2}				
40	1.12×10^{-2}				
30	1.22×10^{-2}				

TABLE 4 Fitting parameters of the cure kinetic model of the $TSPU_7$ formulation

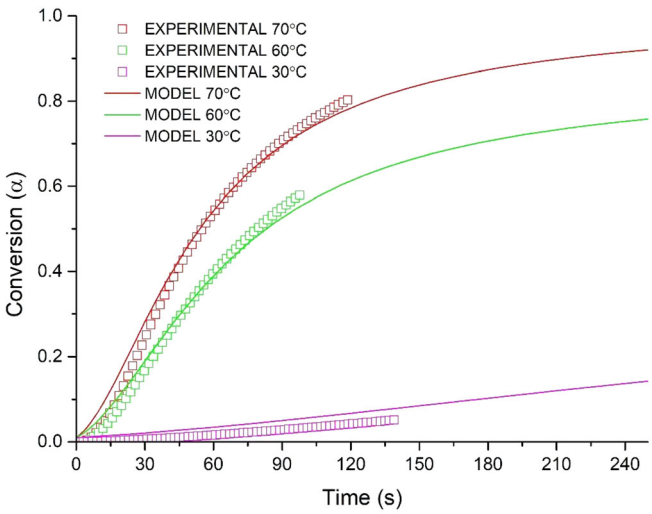

FIGURE 4 Conversion as a function of time comparing the experimental and modeled results of the $TsPU_7$ at isothermal conditions [Color figure can be viewed at wileyonlinelibrary.com]

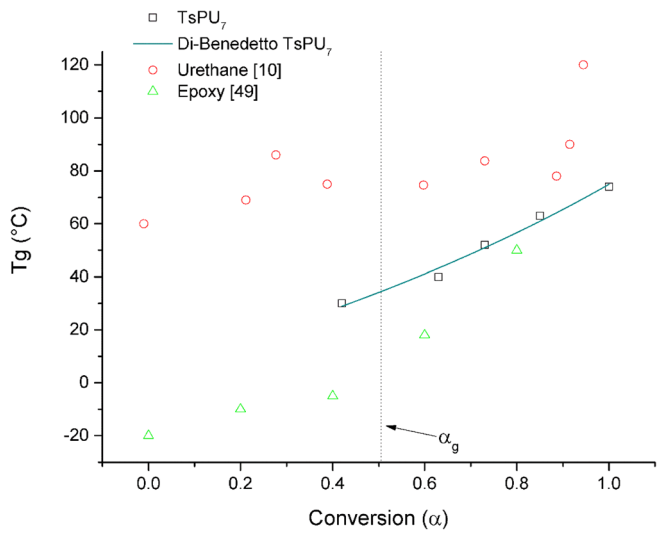

FIGURE 5 Glass to rubbery thermal transition (Tg) as a function of conversion of the $TsPU_7$-70°C [Color figure can be viewed at wileyonlinelibrary.com]

$$k = k_0 exp\left(\frac{E_a}{RT}\right) \tag{3}$$

where k_0 was the pre-exponential factor, E_a is the activation energy, R is the gas constant, and T is the absolute temperature. All the fitting parameters are reported in Table 4 and the comparison between experimental data with the model is depicted in Figure 4.

3.1.2 | Evolution of rubbery to glass transition temperature (T_g) as a function of conversion

To understand how the T_g evolved as a function of conversion, dynamic thermal experiments were performed on samples previously cured at isothermal conditions. The results of these experiments can be depicted in Figure 5, where the evolution of Tg as a function of conversion can be depicted for the $TsPU_7$. The Di-Benedetto equation was used to model the experimental results using the following equation:

$$\frac{T_g - T_{g0}}{T_{g0}} = \frac{\left(\frac{E_\infty}{E_0} - \frac{C_\infty}{C_0}\right)\alpha}{1 - \left(1 - \frac{C_\infty}{C_0}\right)\alpha}, \tag{4}$$

where T_{g0} indicated the transition temperature of the initial monomers in the system, α the extent of reaction (conversion), E_α/E_0 lattice energy of cross-linked and partial cross-linked polymer ratio and C_α/C_0 the segment mobility ratio.

The evolution of T_g as a function of conversion is a key aspect to understand the role of vitrification on the cure of a thermosetting polymer.[43] From a processing point of view, the occurrence of vitrification represents a drawback, because it limits the maximum conversion during cure, affecting the final mechanical properties of the polymer under analysis. A glassy state during cure will certainly indicate that a post-cure cycle should be implemented, so as to attain the maximum Tg of the thermosetting polymer. However, vitrification can also be used to induce a cure inhibition effect, due to the fact that the glassy state inhibits the formation of covalent bonds within the reactive mixture. Further details about

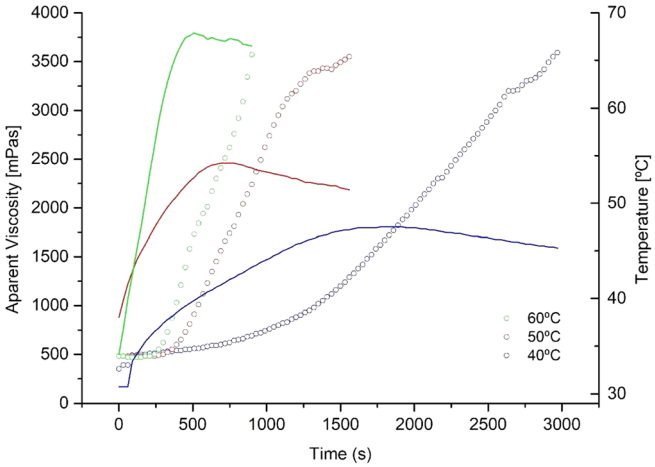

FIGURE 6 Apparent viscosity and in-situ temperature as a function of time for experiments performed at isothermal condition of the $TsPU_7$ formulation [Color figure can be viewed at wileyonlinelibrary.com]

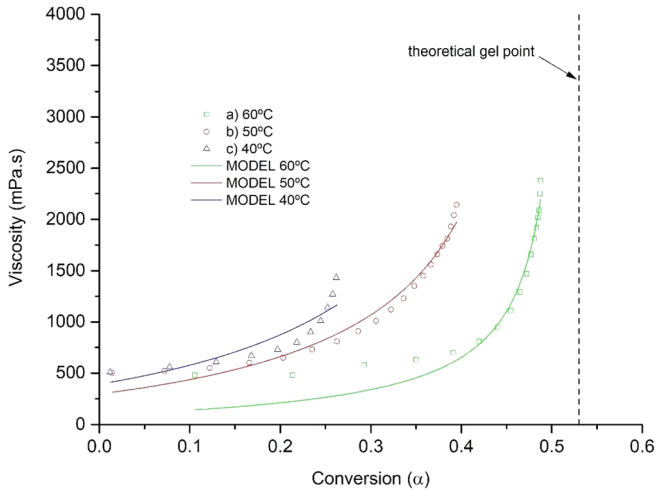

FIGURE 7 Apparent viscosity as a function of conversion for experiments performed at isothermal conditions of the $TsPU_7$ formulation [Color figure can be viewed at wileyonlinelibrary.com]

the role of vitrification on poly(urethane-isocyanurate) thermosets can be consulted in a previous study of our group.[44]

To compare the results in this work with others in literature, we have incorporated in Figure 5 the evolution of Tg as a function of conversion for poly(urethane-isocyanurate)[44] and anhydride cured epoxy systems.[45] For a fixed conversion, that is, 40%, we can deduce that the Tg of the polyurethane systems were much higher with respect to epoxy. This tendency was also found for the case of low conversions, but, for conversions above 80%, the T_g's converged to similar values. These observations clearly reflect how vitrification influences the cure of polyurethane and epoxy systems. Whenever a thermosetting polymer presents a T_g versus conversion curve shifted upwards, then, it is expected that vitrification will certainly inhibit cure. This is because the gelation process is much slower in comparison to the formation of molecular chains which can undergo vitrification at the curing temperatures. Hence, it is also expected that the final cure of the polymer will also take much more time, because the chemical reactions are mostly taking place under a glassy state. However, this effect can also be used to inhibit cure, an aspect which is fundamental for the development of prepregs.[46–48]

3.1.3 | Chemorheological behavior of the TsPU7

The apparent viscosity as a function of time for isothermal experiments of the $TSPU_7$ formulations are depicted in Figure 6. For an isothermal experiment at 40°C, the initial apparent viscosity ranged at 5×10^2 mPa.s and started to increase significantly after 25′, reaching 3.10^3 mPa.s at approximately 45′. In contrast, the isothermal experiment at 60°C yielded an apparent viscosity of 3.10^3 mPa.s at only 12.5′. To better understand the evolution of apparent viscosity as a function of conversion, the results depicted in Figure 7 were modeled using the following equation, proposed originally by Kim and Macosko,[42]

$$\eta(T,\alpha) = \eta(T)\left(\frac{\alpha_g}{\alpha_g - \alpha}\right)^{a+b\alpha}, \tag{5}$$

where "α_g" was the theoretical gel point ($\alpha_g = 0.533$), "a" and "b" are fitting parameters and the function η(T) has an Arrhenius dependence as indicated in the following equation:

$$\eta(T) = \eta_0 e^{\left(\frac{E_{a,M}}{RT}\right)}, \tag{6}$$

where η_0 was the pre-exponential factor, and $E_{a,M}$ is the activation energy, R is the gas constant and T is the absolute temperature. The fitting parameters obtained from the experimental results are reported in Table 5.

A very important deduction from Figure 7 has to do with the role of vitrification and gelation in the evolution of apparent viscosity. For example, for the case of an isothermal experiment at 40°C, from Figure 7 it can be understood that at a conversion of approximately 0.25, the increase of apparent viscosity steeped up significantly. Due to the fact that the theoretical gelation point

TABLE 5 Fitting parameters obtained by the rheological model of $TSPU_7$.

α_g	η_0 [mPa.s]	$E_{a,M}$ [kJ.Mol-1]	a	b
0.528	$2.538.10^{-5}$	61.43	2.00	−1.58

was located at much higher conversions (0.53), it can be deduced that vitrification played the most important role in the increase of apparent viscosity. These results support what has been found in the previous sections, that is, vitrification was the main cause of the observed steep increase in the apparent viscosity. Then, it is logical that the subsequent post-cure cycles should be performed so as to achieve higher chemical conversions.

Another important aspect which needs to be discussed has to do with mass transfer effects. On the one hand, cure reactions are exothermic, so, it is expected that heat flow will have to be dissipated according to the specific geometry of the experiment being conducted. If a high area per unit volume experiment is performed, a lower adiabatic medium shall be present and the material would maintain its original reaction temperature. On the other hand, if isothermal experiments are performed, heat exchange will inevitable affect the reaction kinetics of the polymer system being analyzed.[43] These effects have been extensively studied in literature, but it is important to emphasize the fact that it will inevitably affect any rheological experiment being implemented. For example, in this work, we can deduct from the in-situ temperature measurements (Figure 6) that mass effects contributed to an increase in the time to reach the specific isothermal temperature that was previously established. It might be argued that a different sample mass should be implemented to avoid this, the experiments were performed according to standard recommendations regarding the measurement of apparent viscosity of thermosetting polymers. It is extremely important to report the results presented in Figure 6 and Figure 7 because those are crucial for the application of this thermosetting in polymer composites. From a strictly modeling point of view, it is clear that a parallel plate rheometer[49] will provide a much better set of experimental data, but we also think it is very important to conduct and report rotational experiments because these are widely employed in industry.

3.2 | The role of catalyst type and concentration on the cure of the TsPU

The effect of catalyst type and concentration was analyzed from the exothermic thermal transitions identified by performing dynamic thermal scans using the DSC analysis. These events were quantified by indicating the position of the thermal event (exothermic peak temperature) and the total enthalpy associated with it (ΔH_T). The results of these analyses are reported in Table 6. For the case of the $TsPU_1$, an exothermic event centered at 80°C with an enthalpy of 3.32 $J.g^{-1}$ was identified. The position as well as the enthalpic value clearly suggested that the SOYPOL had a low reactivity, an aspect which can be explained by the fact that the hydroxides present in the polyol are secondary and that the oxirane rings also contribute to a strong steric hindrance effect.[8] If the ΔH_T is expressed as a function of isocyanate equivalents (see Table 6), we can also notice that the value is well below the heat of reaction of typical isocyanate-hydroxyl reactions reported in the literature.[42,50] This result was expected and it can be explained by the absence of a catalyst in the formulation as well as the low reactivity of the SOYPOL. FTIR analysis (Figure 8) of the $TsPU_1$ revealed the presence of urethane bonds, hydroxides and free isocyanates, supporting the hypothesis that those reactions had occurred, but to a lesser extent.

The effect of increasing amounts of DMCHA on the cure enthalpy of the formulation is also reported in Table 6. The thermal transition shifted to higher temperatures[51] and the ΔH_T increased by +174% (for a 0.9 wt% of DMCHA), indicating that the catalyst was effective in increasing the catalytic activity of the formulation. This fact clearly suggested that the formulation was capable of producing reactions which might not be only associated with urethane linkages. For temperatures above 100°C, a wide variety of reactions between isocyanate groups are feasible.[8] This hypothesis was corroborated by the FTIR analysis (Figure 8), which corroborated the presence of isocyanurate, urea and other chemical bonds typically found in such formulations.

The effect of incorporating DBTDL in the formulation is reported in Table 6 ($TsPU_5$). At only 0.2 wt%, the thermal transition shifted to much lower temperatures and the ΔH_T also increased to similar levels of the $TsPU_4$ formulation. This fact clearly indicated that this catalyst was much more effective at lower concentrations, a result which was also expected.[36]

The effect of incorporating glycerin in the formulation catalyzed with DBTDL is reported also in Table 6 ($TsPU_6$, $TsPU_7$, and $TsPU_8$). A substantial increase of the ΔH_T was measured, reaching a value of 35.7 $J.g^{-1}$. Taking into account that this formulation had the highest amounts of hydroxide equivalents, it was logical to obtain those results. In addition, the ΔH_{TNCO} (enthalpy normalized with respect to isocyanate equivalents) was also the highest, indicating that the role of urethane linkages was predominant for the formation of a crosslinked network.

TABLE 6 Results of the dynamic scans for the formulations used in this work.

Formulation	ΔH_T [J.g^{-1}]	ΔH_{TNCO} [J.eq^{-1}]	Peak temperature [°C]
$TsPU_1$	$3.32.10^0 \pm 0.6$	$1.68.10^3 \pm 0.6$	$7.98.10^1 \pm 1.76$
$TsPU_2$	$4.27.10^0$	$2.16.10^3$	$1.38.10^2$
$TsPU_3$	$4.65.10^0$	$2.35.10^3$	$1.38.10^2$
$TsPU_4$	$9.09.10^0$	$4.60.10^3$	$1.38.10^2$
$TsPU_5$	$9.06.10^0 \pm 0.95$	$4.60.10^3 \pm 0.95$	$3.32.10^1 \pm 3.48$
$TsPU_6$	$1.36.10^1 \pm 5.2$	$7.89.10^3 \pm 5.2$	$3.55.10^1 \pm 1.4$
$TsPU_7$	$3.57.10^1 \pm 3.45$	$9.45.10^3 \pm 3.45$	$3.76.10^1 \pm 2.68$
$TsPU_8$	$3.09.10^1$	$7.25.10^3$	$3.85.10^1$

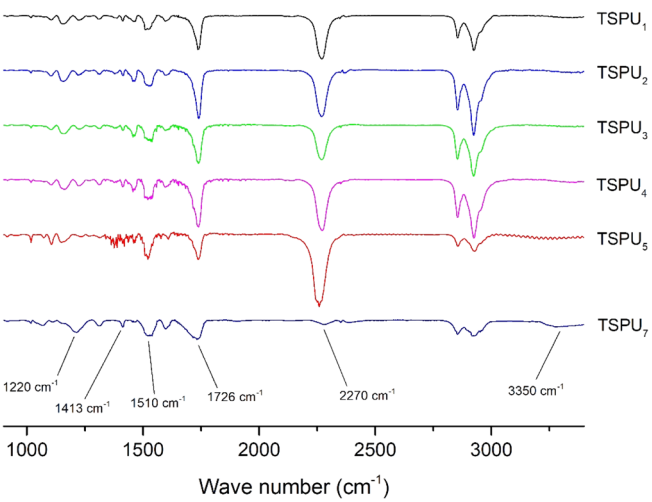

FIGURE 8 FTIR analysis of the TsPU formulations used in this work [Color figure can be viewed at wileyonlinelibrary.com]

The effect of isocyanate index (NCO_{index}) is also reported in Table 6. It is important to highlight that the index effect was based on the $TsPU_7$ formulation. By reducing the index to 0.31, we found a 62% decrease of the ΔH_T, clearly indicating that the formulation had a deficit of isocyanate equivalents. On the other hand, an increase of the NCO_{index} to 1.37 also caused a 13.4% decrease of the ΔH_T, indicating an excess of isocyanate equivalents. Taking into account these results, it is logical to deduce that the proposed $TsPU_7$ formulation had an adequate stoichiometric relation, giving rise to a balance of hydroxides as well as isocyanate equivalents. This is further confirmed by the ΔH_{TNCO}, which was the highest of all the tested formulations. Furthermore, as it can be deduced from the FTIR spectrum of cured samples of the $TsPU_7$ (Figure 8), the free isocyanate absorption band centered at 2270 cm^{-1} was almost vanished, suggesting that the material attained a full cure.

Finally, it is important to comment on the specific values of ΔH_{TNCO} measured for all the formulations. In scientific literature,[41,52] and, in particular, when model systems are under analysis, the total reaction enthalpy is normalized with respect to the isocyanate or hydroxides equivalents. The main purpose of this normalization is to compare the enthalpies for the formation of a urethane bond. For example, several studies have indicated that, for model systems, the urethane bond formation should be 83.6×10^3 J mol^{-1}.[42,50] Then, by analyzing the results reported in Table 6, it might be argued that the values reported are far below what has been established by the previous works. However, it is important to highlight that not only urethane bonds are being formed in the $TsPU_7$ formulation. As already discussed above and supported by FTIR analysis (Figure 8), other chemical bonds were present, which might be associated with lower formation energies. Another important aspect of this formulation has to do with the role of the rubber to glass transition temperature (Tg). As it will be explained in detail in the following section, this formulation had a cure kinetics which was substantially hindered by diffusion effects. This meant that it was logical to have a low ΔH_{TNCO} during cure, because such systems tend to have very long post-cure cycles. This hypothesis was also supported by the results presented in Section 3.3.

3.3 | The role of polyol crystallization on cure kinetics

The crystallization of the SOYPOL was visually identified after samples were stored at temperatures ranging from −18°C to approximately 4°C. The visual formation of crystals for the SOYPOL as well as the SOYPOL formulated with glycerin are depicted in Figure 9. To further understand this phenomena, a series of experiments were performed studying the effect of temperature on crystallization. The polyols reported in Table 2 were stored at temperatures within the range of −18°C to 14°C for periods of time ranging from 15 days to 180 days. Subsequently, samples of those conditioned polyols were analyzed with DSC using a standard dynamic thermal scan so as to identify melting endotherms. For example, for

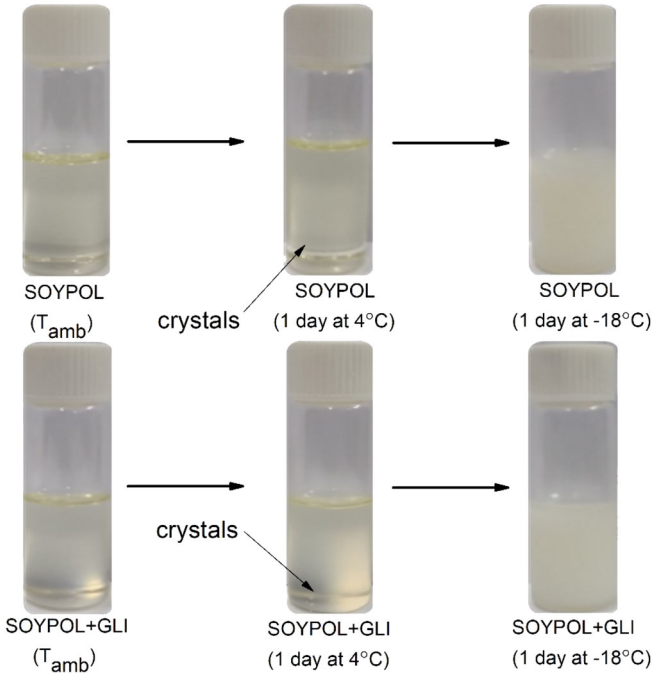

FIGURE 9 Crystallization of the SOYPOL (a, b and c) and SOYPOL + glycerin (d, e and f) [Color figure can be viewed at wileyonlinelibrary.com]

the case of the SOYPOL stored at 4°C for 180 days, an endotherm centered at 44°C and with a total endothermic enthalpy of 4.74 $J.g^{-1}$ was measured.

The presence of a melting endotherm centered at temperatures well above ambient temperature clearly suggested that polyol crystallization could have a strong effect on cure kinetics.

Due to the fact that the SOYPOL used in this work was synthesized from an epoxidation reaction, it is possible that the unreacted oxirane groups present in the molecular structure of the SOYPOL might lead to macromolecular crystallization.[52] This phenomenon has previously been identified by other studies,[52,53] however, all the melting transitions were found well below −10°C, indicating that this phenomenon was relevant only for very low temperatures. It is important to highlight that the authors have not found kinetic studies which quantify the crystallization nor melting of such polyols. We have only found the similar studies for epoxy precursors.[54–56]

At this point, it is important to emphasize the relevance of understanding the concept that crystallization can have a deleterious impact on the final properties of a TsPU. For example, if a polyol that has been partially crystallized is used in the formulation, this means that, under this condition, the polyol will have a lower OH#. This is because the crystals behave as a second solid phase with a very low reactivity toward the isocyanate

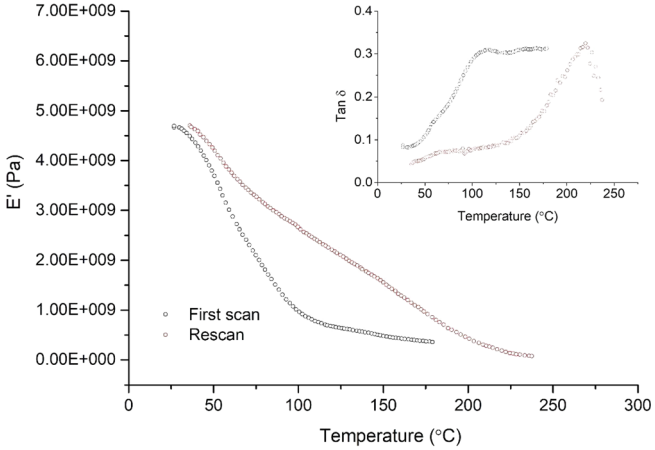

FIGURE 10 Elastic modulus and damping factor (tan δ) as a function of temperature of the $TsPU_7$. A first scan and re-scan of the same sample was performed [Color figure can be viewed at wileyonlinelibrary.com]

precursor. The consequence is that the polyurethane formulation will have a higher NCO_{index}, because less hydroxides groups will be available to react with the isocyanate precursor. In addition, due to the fact that the polyurethane cure generates heat, the crystals will melt, giving rise to localized zones with incomplete cure. Such phenomena will certainly adversely affect the thermomechanical properties of the resultant TsPU.

3.4 | Dynamic mechanical analysis (DMA)

The elastic bending modulus (E') as well as the damping factor (tan δ) as a function of temperature for the $TsPU_7$ formulation are depicted in Figure 10. The sample $TsPU_7$−1 was obtained from a plate cured at an ambient temperature. After this thermal cycle was conducted, the same sample was subjected to a second thermal cycle, denominated as $TsPU_7 - 2$. For the case of the $TsPU_7 - 1$, the storage bending modulus (E') had a substantial decrease as a function of temperature, starting at $4.66.10^9$ Pa at ambient temperature and going down to $3.58.10^8$ Pa at 180°C. In addition, the damping factor (tan δ) presented a thermal transition centered at approximately 100°C. However, this transition was not clearly defined, indicating that the sample was curing when the analysis was being conducted. On the other hand, for the case of the $TsPU_7$-2, a clearly defined thermal transition (Tg) was found at approximately 220°C, indicating that the material attained a higher conversion. In addition, the residual storage elastic modulus was $6.7.10^7$ Pa, indicating that only a 1.3% of the initial E′ was retained at 240°C.

It is important to highlight that, as already mentioned in the previous section, vitrification inhibited substantially the final conversion of the TsPU. When a sample is obtained from an unheated mold, it is logical to expect that a post-cure cycle will be necessary to achieve improved thermo-mechanical properties. We chose to conduct these experiments intentionally so as to highlight the impact of vitrification on the thermo-mechanical properties of the $TsPU_7$.

Unfortunately, we cannot compare the results obtained in this section with others in the literature. DMA analysis of a similar thermosetting has not been reported before. However, there are studies which serve as a baseline for comparison. Tan et al.,[49] studied the thermomechanical properties of thermosettings based solely on ESO thermally cured with methylhexahydrophtalic anhydride (MHHPA). DMA analysis showed that a Tg ranging from 53°C to 70°C was obtained. An early study of Husic et al.[57] used a formulation based on a low OH# polyol (commercial name Soypolyol 204) crosslinked with a petrochemical triol (Jeffol G30-650). DMA results indicated that the Tg was approximately 140°C. Several studies can be found within the area of PU thermosets using acrylated variants (AESO) obtained from soybean oil.[58–61] These thermosets have been successfully applied as a matrix for natural-fiber reinforced polymer composites, especially with flax fibers. For example, Adekunle et al.[44,58] prepared thermosets reinforced with flax fibers as well as glass/flax hybrids with T_g's oscillating at around 100°C. However, the main drawback of AESO had to do with the fact that styrene was usually employed so as to improve reinforcement impregnation.

3.5 | Quasi-static flexural mechanical tests

The results of the flexural mechanical tests performed on samples of the $TsPU_7$ post-cured at 70°C ($TsPU_7$ – 70°C) and 110°C ($TsPU_7$ – 110°C) are reported in Table 7. The flexural strengths attained under both conditions were similar, with a maximum value of 99.4 MPa for the case of the sample cured at a higher temperature. The flexural modulus had a strong change as a function of post-cure cycle, increasing by up to 24% to 2.14 GPa for the case of the $TsPU_7$–110°C. In addition, the standard deviation of the flexural modulus decreased substantially as a function of higher post-cure cycle temperatures.

This was a clear indication that supported the hypothesis that vitrification was playing a key role in the post-cure of this thermosetting formulation. For this reason, higher temperatures were needed in order to attain full cure and, subsequently, to homogenize the mechanical properties of the material under analysis.

Finally, the flexural strain to failure was also highly dependent on the post-cure cycle, decreasing by up to 30% to 5.69% for the case of high-temperature post-cure cycle.

This last result also reflected the fact that subsequent crosslinking took place under the post-cure cycle. Such effect was expected due to the fact that the initial crosslinking of the low OH# polyol (ESO) caused vitrification (see Section 4.2), decreasing substantially the rate of reaction of the OH groups present in the glycerin polyol.

Similarly, to the previous sections, it is difficult to compare the results presented in this work with analogs reported previously in literature. Fu et al.[62] studied thermosets obtained from AESO with tensile strength's below 40 MPa. Triolein[63] based polyurethanes gave a tensile strength of 8.7 MPa with a Tg ranging around 25°C. Husic et al.[57] reported a flexural strength of 418 MPa for the case of a glass reinforced soy-based composite. Adekunle et al.[58] reported a flexural strength below 118 MPa and flexural modulus ranging from 4 to 6 GPa for the case of flax reinforced AESO thermosets.

4 | CONCLUSIONS

A thermosetting polyurethane was synthesized by combining an aromatic isocyanate and a polyol obtained from soybean oil using ESO crosslinked with glycerin. Cure kinetics analysis with DSC revealed that DBTDL was the most effective catalyst for the proposed formulation, with a total reaction enthalpy of 35.7 J g^{-1}. Aminic catalysts improved reaction kinetics, but to a lesser extent. DSC analysis were able to corroborate that a proper NCO_{index} was selected, maximizing the reaction enthalpy for the proposed formulation. A cure kinetics model based on autocatalytic heat flow where vitrification was preponderant in the evolution of conversion was obtained. FTIR analysis of cured samples corroborated the formation of both urethane as well as isocyanurate and urea bonds. In addition, the proposed $TsPU_7$ formulation presented a

TABLE 7 Quasi-static flexural properties of the $TsPU_7$.

Material	Flexural strength (MPa)	Flexural modulus (GPa)	Flexural strain to failure (%)
$TsPU_7$–70°C	90.7 ± 18.1	1.73 ± 0.537	8.10 ± 1.69
$TsPU_7$–110°C	99.42 ± 13.93	2.14 ± 0.0455	5.69 ± 1.37

very weak absorption band centered at 2270 cm^{-1}, indicating that full cure was attained. The evolution of T_g's as a function of temperature substantiated that vitrification slowed down cure kinetics, particularly at isothermal experiments performed at lower temperatures (<60°C). ESO crystallization was induced and quantified with DSC, finding a melting endotherm well above room temperature. This clearly indicated that ESO crystallization might have a strong effect on cure kinetics. DMA analysis of cured and in-situ post-cured samples revealed that a T_g centered at 220°C was attained. Quasi-static flexural mechanical tests proved that post-cure cycles had a strong effect on flexural modulus, strain to failure and strength. A maximum flexural modulus of 2.14 GPa was obtained for the highest post-cure cycle temperature (110°C) and a maximum strain to failure of 8.14% was obtained for the lowest one (70°C).

The previous results are key to extending and promoting the use of biobased thermosetting polymers, particularly in the polymer composite industry. This will certainly aid to develop sustainable solutions within this industry, aiding toward a more circular economy. Ongoing work in this area will focus on the effect of changing the amounts of crosslinking on the thermomechanical properties of the resultant thermosetting polymers, focusing on the role of cure and post-cure cycles.

AUTHOR CONTRIBUTIONS

Franco Armanasco: Conceptualization (equal); data curation (lead); methodology (lead). **Sebastian D'hers:** Investigation (equal); methodology (supporting); resources (equal); **Leonel Matías Chiacchiarelli:** Data curation (supporting); conceptualization (lead); funding acquisition (lead); investigation (lead); original draft (lead); resources (lead).

ACKNOWLEDGMENTS

The authors appreciate the advice and support from Matias Ferreyra (Huntsman), Diego Judas (Alkanos) and Hernan Bertolotto (Mayerhofer Argentina S.A.). The work was funded by the "PICT 2015 N0475," ANPCYT (Argentina) as well as the "PIP-2015-N0425," supported by CONICET.

DATA AVAILABILITY STATEMENT

The data that support the findings of this study are available on request to the corresponding author.

ORCID

Franco Armanasco https://orcid.org/0000-0003-1221-2994
Sebastián D'hers https://orcid.org/0000-0002-4979-8813
Leonel Matías Chiacchiarelli https://orcid.org/0000-0002-7342-1784

REFERENCES

[1] L. M. Chiacchiarelli, *Pages* **2019**, *1*, 135.
[2] M. Desroches, M. Escouvois, R. Auvergne, S. Caillol, B. Boutevin, *Polym. Rev.* **2012**, *52*, 38.
[3] A. Fridrihsone, F. Romagnoli, V. Kirsanovs, U. Cabulis, *J. Cleaner Prod.* **2020**, *266*, 121403.
[4] S. Miao, P. Wang, S. Zhiguo, S. Zhang, *Acta Biomater.* **2014**, *10*, 1692.
[5] S. Zoran, Petrovi'c., *Polym. Rev.* **2008**, *48*, 109.
[6] Y. Xia, R. C. Larock, *Green Chem.* **2010**, *12*, 1893.
[7] S. Zoran, I. J. Petrovi'c, M. Ionescu, *J. Renew. Mater.* **2013**, *1*, 167.
[8] M. Ionescu, *Chemistry and Technology of Polyols for Polyurethanes*, Smithers Rapra Publishing, Shrewsbury, England **2005**.
[9] R. Herrán, J. I. Amalvy, L. M. Chiacchiarelli, *J. Appl. Polym. Sci.* **2019**, *136*, 47959.
[10] S. Zoran, A. Z.'c. Petrovi'c, C. C. Lava, S. Sinadinovi'c-Fišer, *Eur. J. Lipid Sci. Technol.* **2002**, *104*, 293.
[11] A. Campanella, M. Baltanas, *Chem. Eng. J.* **2006**, *118*, 141.
[12] A. Campanella, M. Baltanas, *Chem. Eng. Process.* **2007**, *46*, 210.
[13] Alejandrina Campanella, Carina Fontanini, and Miguel Baltanas. *Chem. Eng. J.*, *144*:466–475, **2008**.
[14] E. Santacesaria, R. Turco, V. Russo, R. Tesser, M. Di Serio, *Processes* **2020**, *8*, 1134.
[15] A. F. Aguilera, P. Tolvanen, S. Heredia, M. G. Munoz, T. Samson, A. Oger, A. Verove, K. Eranen, S. Leveneur, J.-P. Mikkola, et al., *Indus. Eng. Chem. Res.* **2018**, *57*, 3876.
[16] S. Szycher, *Handbook of Polyurethanes, Ch.11*, CRC Press, Boca Raton, FL **1999**.
[17] S. Anbinder, C. Meiorin, C. Macchi, M. A. Mosiewicki, M. I. Aranguren, A. Somoza, *Eur. Polym. J.* **2020**, *124*, 109470.
[18] C. Meiorin, T. Calvo-Correas, M. A. Mosiewicki, M. I. Aranguren, M. A. Corcuera, A. Eceiza, *J. Appl. Polym. Sci.* **2020**, *137*, 48741.
[19] C. Esposito Corcione, A. Maffezzoli, *Thermochim. Acta* **2009**, *485*, 43.
[20] D. Czachor-Jadacka, B. Pilch-Pitera, Ł. Byczy'nski, M. Kisiel, A. Zioło, *Prog. Org. Coat.* **2021**, *159*, 106402.
[21] G. Fredi, A. Dorigato, A. Pegoretti, *Polym. Compos.* **2019**, *40*, 3711.
[22] T. Ageyeva, I. Sibikin, J. G. Kovács, *Polymers* **2019**, *11*, 1555.
[23] Kv Van Rijswijk and HEN Bersee, *Compos. Part A: Appl. Sci. Manuf.* **2007**, *38*, 666.
[24] L. M. Chiacchiarelli, I. Puri, D. Puglia, J. M. Kenny, L. Torre, *Thermochim. Acta* **2012**, *549*, 172.
[25] J. M. Kenny, A. Maffezzoli, L. Nicolais, *Compos. Sci. Technol.* **1990**, *38*, 339.
[26] A. Terenzi, J. M. Kenny, G. Lelli, L. Torre, *Polym. Compos.* **2009**, *30*, 1.
[27] A. Maffezzoli, A. Trivisano, M. Opalicki, J. Mijovic, J. M. Kenny, *J. Mater. Sci.* **1994**, *29*, 800.
[28] S. Mazumdar, *Composites Manufacturing: Materials, Product, and Process engineering*, CRC press, London, UK **2001**.
[29] P. K. Mallick, *Fiber-Reinforced Composites: Materials, Manufacturing, and Design*, CRC Press, London, UK **2007**.
[30] L. M. Chiacchiarelli, J. M. Kenny, L. Torre, *Thermochim. Acta* **2013**, *574*, 88.

[31] M. A. Esperanza Díaz, I. I. Marín, I. Irastorza, *J. Maritime Res.* **2011**, *8*, 59.
[32] A. C. Milanese, M. O. H. Cioffi, H. J. C. Voorwald, C. Y. Shigue, *J. Appl. Polym. Sci.* **2011**, *122*, 3168.
[33] E. Papadopoulos, M. Ginic-Markovic, S. Clarke, *J. Appl. Polym. Sci.* **2009**, *114*, 3802.
[34] J. M. E. Rodrigues, M. R. Pereira, A. G. De Souza, M. L. Carvalho, A. A. Dantas Neto, T. N. C. Dantas, J. L. C. Fonseca, *Thermochim. Acta* **2005**, *427*, 31.
[35] M. C. Saha, B. Barua, S. Mohan, *J. Eng. Mater. Technol.* **2011**, *133*, 011015.
[36] D. Randall, S Lee. *The Polyurethanes Book*, New York **2002**.
[37] H. Sardon, A. Pascual, D. Mecerreyes, D. Taton, H. Cramail, J. L. Hedrick, *Macromolecules* **2015**, *48*, 3153.
[38] J. H. Marciano, A. J. Rojas, R. J. J. Williams, *Polymer* **1982**, *23*, 1489.
[39] O. Yuksel, M. Sandberg, I. Baran, N. Ersoy, J. H. Hattel, R. Akkerman, *Compos., B* **2021**, *207*, 108543.
[40] E. Poodts, G. Minak, E. Dolcini, L. Donati, *Compos., B* **2013**, *53*, 179.
[41] J. M. Castro, C. W. Macosko, *AIChE J.* **1982**, *28*, 250.
[42] C. W. Macosko, *RIM, Fundamentals of Reaction Injection Molding*, Hanser Publishers, Liberty Township, Ohio **1989**.
[43] H. Teil, S. A. Page, V. Michaud, J.-A. E. Månson, *J. Appl. Polym. Sci.* **2004**, *93*, 1774.
[44] K. Adekunle, D. Åkesson, M. Skrifvars, *J. Appl. Polym. Sci.* **2010**, *115*, 3137.
[45] J. P.-H. Belnoue, O. J. Nixon-Pearson, D. Ivanov, S. R. Hallett, *Mech. Mater.* **2016**, *97*, 118.
[46] T. Centea, L. K. Grunenfelder, S. R. Nutt, *Compos Part A: Appl. Sci. Manuf* **2015**, *70*, 132.
[47] Z. Tuncay, C. Cron, M.-E. Schmidt, S. Poehler, B. Sanitther, T. Troester, *Int. J. Autom. Compos.* **2018**, *4*, 71.
[48] J.-P. Pascault, H. Sautereau, J. Verdu, R. J. J. Williams, *Thermosetting Polymers*, CRC Press, Boca Raton, Florida **2002**.
[49] S. G. Tan, W. S. Chow, *Exp.Polym. Lett.* **2011**, *5*, 480.
[50] Y. Zhao, G. Suppes, *Polym. Eng. Sci.* **2015**, *55*, 4.
[51] S. D. Lipshitz, C. W. Macosko, *J. Appl. Polym. Sci.* **1977**, *21*, 2029.
[52] B. Lin, L. Yang, H. Dai, A. Yi, *J. Am. Oil Chem. Soc.* **2008**, *85*, 113.
[53] Z. S. Petrović, L. Yang, et al., *J. Appl. Polym. Sci.* **2007**, *5*, 2717.
[54] R. J. Morgan, O'neal, J. E., *J. Macromol. Sci., Part B: Phys.* **1978**, *15*, 139.
[55] F. Ali, Y. W. Chang, S. C. Kang, J. Y. Yoon, *Polym. Bull.* **2009**, *62*, 91.
[56] C. Sarathchandran, L. Ziang, R. A. Shanks, C. H. Chan, V. Sekkar, S. Thomas, *J. Therm. Anal. Calorim.* **2020**, *141*, 727.
[57] S. Husić, I. Javni, Z. S. Petrović, *Compos. Sci. Technol.* **2005**, *65*, 19.
[58] K. Adekunle, D. Åkesson, M. Skrifvars, *J. Appl. Polym. Sci.* **2010**, *116*, 1759.
[59] E. Can, R. P. Wool, S. Küsefoğlu, *J. Appl. Polym. Sci.* **2006**, *102*, 1497.
[60] K. Adekunle, S. W. Cho, R. Ketzscher, M. Skrifvars, *J. Appl. Polym. Sci.* **2012**, *124*, 4530.
[61] K. Liu, S. A. Madbouly, M. R. Kessler, *Eur. Polym. J.* **2015**, *69*, 16.
[62] L. Fu, L. Yang, C. Dai, C. Zhao, L. Ma, *J. Appl. Polym. Sci.* **2010**, *117*, 2220.
[63] A. Zlatanić, Z. S. Petrović, K. Dušek, *Biomacromolecules* **2002**, *3*, 1048.